ASSOCIAZIONE NAZIONALE ITALIANA DI INGEGNERIA SISMICA
ANIDIS
Italian National Association of Earthquake Engineering

XVIII CONVEGNO ANIDIS
L'ingegneria sismica in Italia
ASCOLI PICENO 2019
15-19 Settembre

Damage detection and optimal sensor placement in health monitoring of "Collegiata di Santa Maria" in Visso (Central Italy)

Ersilia Giordano[a], Francesco Clementi[a], Alberto Barontini[b], Maria-Giovanna Masciotta[b], Eleni Chatzi[c], Luis F. Ramos[b], Paulo Amado-Mendes[b]

[a] *Polytechnic University of Marche, Department of Civil and Building Engineering, and Architecture, Ancona, Italy*
[b] *ISISE, University of Minho, Department of Civil Engineering, Guimarães, Portugal*
[c] *Institute of Structural Engineering, ETH Zürich, Zürich, Switzerland*

Keywords: Structural health monitoring; cultural heritage; masonry structures; optimal modal analysis; optimal sensor placement;

ABSTRACT

Seismic protection and vulnerability reduction are very relevant issues in European regions, such as Italy, characterized by the presence of a large stock of cultural heritage structures. This concern increased the interest in Structural Health Monitoring (SHM) as a powerful tool to quantify and reduce uncertainties regarding the structural performance of buildings. Vibration-based monitoring can be successfully implemented in some cases to assess the real need for structural interventions or to control the medium -and long- term effectiveness of already applied strengthening solutions. In this paper, dynamic identification techniques are applied to the case study of the Collegiata of Santa Maria in Visso (Macerata Province, Marche Region) heavily damaged by the Central Italy seismic sequence of 2016. In addition, a deterministic approach for Optimal Sensors Placement (OSP)is employed in order to identify how properly place the accelerometers to maximize the quality of SHM information with the minimum number of sensors, aiming at driving the future long-term monitoring of the church.

1 INTRODUCTION

In October 2016 – two months after the first seismic sequence – a series of major earthquakes hit again Central Italy causing widespread damage to the existing building stock as well as social and economic losses (Francesco Clementi, Ferrante, Giordano, Dubois, & Lenci, 2019; Giordano, Clementi, Nespeca, & Lenci, 2019). This second seismic sequence struck Norcia, Preci, and Visso, the municipality of the Marche region in which the "Collegiata of Santa Maria" investigated in this paper is located. The main aim of this research is the dynamic characterization of this historical masonry construction in light of the structural damage caused by the quake, using both experimental and numerical studies (Cavalagli, Comanducci, & Ubertini, 2018; F. Clementi, Pierdicca, Formisano, Catinari, & Lenci, 2017; Ferraioli, Miccoli, & Abruzzese, 2018; Masciotta, 2018; Pierdicca et al., 2016). The experimental investigation was based on ambient vibration tests, while the numerical study relied on finite element analysis with solid elements. First of all, the results of the experimental campaign were used to calibrate the numerical model of the structure. As the most doubtful parameters, the modulus of elasticity of the masonry and the interaction among structural parts were adjusted by simple operations to achieve a reasonable tuning between measured and simulated response. Once a good consistency between experimental and numerical results was obtained, the study revealed the actual dynamic properties of the damaged church. Taking advantage of this information, a deterministic-based approach was finally applied to define the optimal number and position of accelerometers in view of the future long-term monitoring of the church using a limited but cost-efficient spatial distribution of sensors. This technique is known as Optimal Sensor Placement (OSP) and it consists in designing the most

appropriate sensor system network, by defining the optimal combination of type, number and location of accelerometers under some performance metrics and tailored to the specificity of the structure analyzed (Capellari, Chatzi, & Mariani, 2018; Guo, Zhang, Zhang, & Zhou, 2004; Li, Li, Zhao, & Ou, 2012; Worden & Burrows, 2001). Different performance metrics are used to determine the optimal sensor placement for the case study under investigation, dealing with the development of a new damage detection method that can exploit data from an optimized set of accelerometers locations. To maximize the quality of the information collected while reducing data overflow and operating costs, OSP becomes a necessary task in the design of health monitoring systems.

2 THE CASE STUDY

2.1 Historical development

The Collegiata's origins date back to 1143 when a little chapel was built against a water mill to venerate the Madonna Bruna. Indeed, in the past, the Nera river flowed in this place. At the beginning of the XIII century the population moved to the down and the river was diverted; thus, a parish church with a little bell tower was built in place of the little chapel.

Over the years the population grew so much that it was necessary to add another church to the parish church. The new church was built without apse, which was added only in 1312. In the same period, the bell tower spire was also constructed (Figure 1). Between 1324 and 1332, a stone door and a portico were built in the North-West façade, but the latter was demolished in 1572.

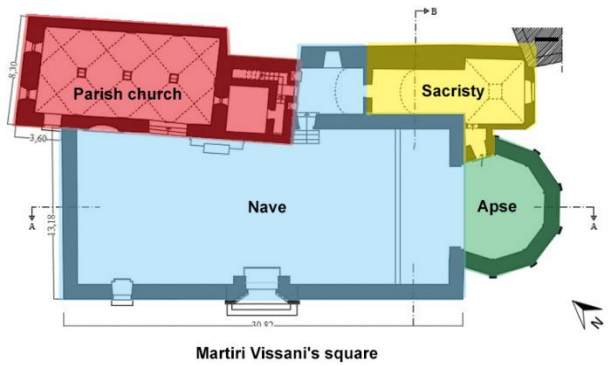

Figure 1. Historical evolution of Collegiata of Visso. XIII century: old parish church and bell tower (red); XIV century: new church with sacristy (blue) and apse (green); XVIII century: new sacristy (yellow).

2.2 Geometrical survey

The Collegiata features a Romanic-Gothic style and consists of four main blocks: (i) the church, (ii) the sacristy, (iii) the old parish church and (iv) the bell tower. The church has a basilica plan with a single nave of 12 m width, 29 m length and a maximum height of about 14 m, ending with a polygonal apse of 3.70 m radius (Figure 2). As for the materials, the walls of both apse and main façade are made of rubble masonry covered by travertine blocks, the West façade is built in regular limestone stones while the others are made of rose stones. A steel roof truss bridges the space above the nave, while the roof above the apse semi-dome is supported by wooden beams lying on a concrete curb. On the North-West side, an arcade connects the church to the old parish church, which features a pseudo-rectangular plan 13.50 m long and 6.80 m wide, with two naves divided by one row of stone polygonal columns that provide support to the cross vault ceiling, and walls made of irregular stones. On the same side, a door connects the church to the bell tower and the sacristy. The former is located between the parish church and the sacristy, and is characterized by a square plan of 4 m side and a height of 40 m. The latter is located in the North-East side, it has a rectangular plan of 13 x 5 m^2 and consists of two floors, of which the first one is placed at a height of 5 m and is covered by barrel and cross vaults.

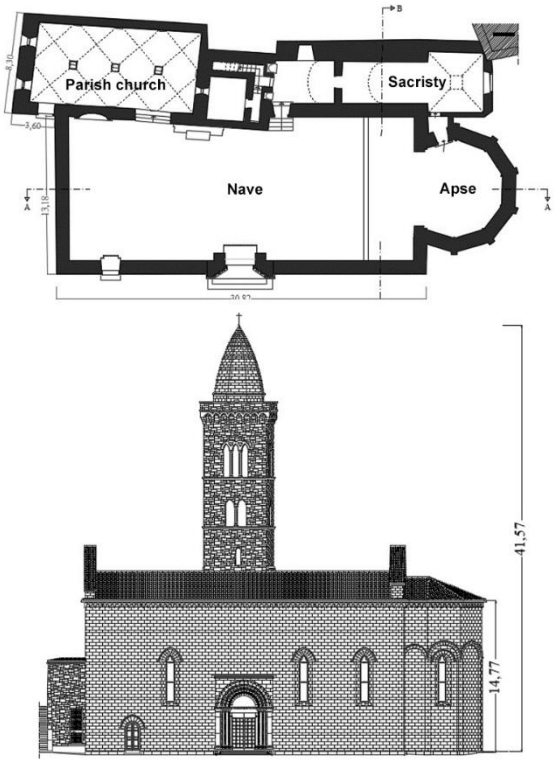

Figure 2. Actual geometrical configuration of Collegiata.

2.3 *The damages of the 2016 Central Italy earthquake*

After the 2016 Central Italy earthquake, the historical complex exhibited serious damages, with spread cracks crossing all the structural walls. A further increase in the width of existing cracks located above the windows of the main façade and apse was visually detected (Figure 2).

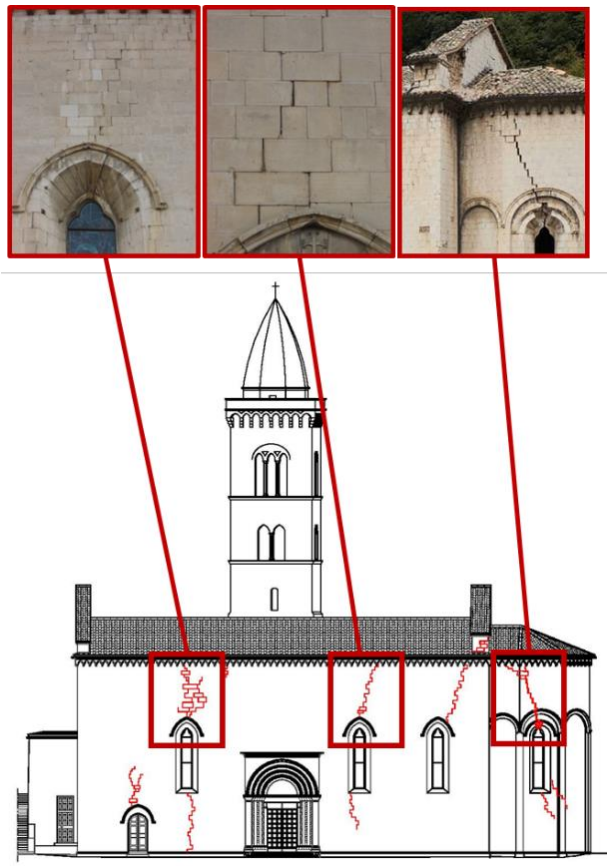

Figure 2 Crack pattern in the South-West façade and apse.

On the North-West side, the onset of an out-of-plane mechanism could be clearly distinguished in correspondence of the cracks arisen between the façade and the orthogonal side wall of the nave. The tower also exhibited extensive damages, with the most serious crack appearing at the connection with the wall nave as a result of the seismic hammering due to the different vibration period of the tower as compared to the one of the adjacent church (Figure 3). As for the vaults, many cracks appeared after the earthquake, especially in the cross vaults of the sacristy and of the semi-dome of the apse.

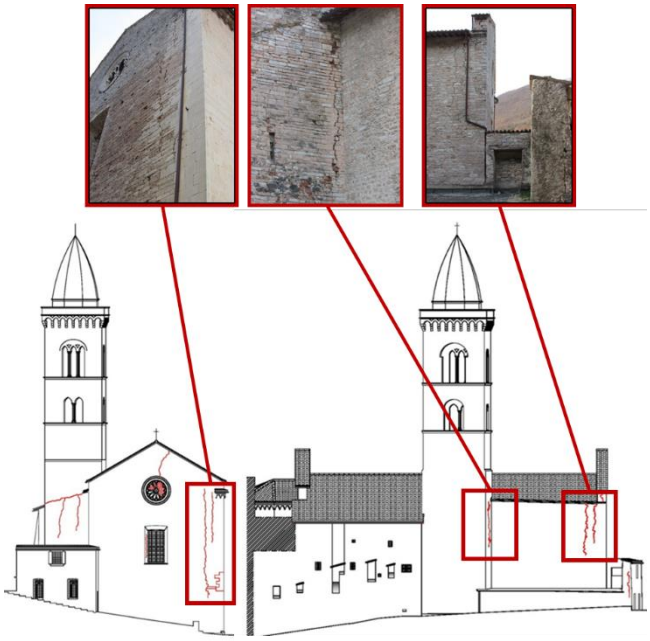

Figure 3 Crack pattern in the North-West and North-East façades.

3 DYNAMIC CHARACTERIZATION

To analyze the structural behavior of complex historical buildings, Finite Element (FE) models are normally recommended to adequately reproduce geometries that could not be otherwise represented by simplified methods (Monni, Clementi, Quagliarini, Giordano, & Lenci, 2017; Quagliarini, Maracchini, & Clementi, 2017). Based on these models, linear and/or nonlinear static and dynamic analysis are then carried out to shed light on the actual response of such buildings under different loading conditions. However, even though the geometry can be accurately reproduced through an FE software, there are crucial input data that can sensibly affect the real behavior of the building under analysis, such as the mesh discretization and the structural damping that is dependent not only on the material parameters, but also on the ongoing damage mechanisms, e.g. opening and closure of micro cracks, which are difficult to represent. To improve the accuracy of the FE model, experimental data can be used as reference information to tune numerical (simulated) and real (measured) behavior. In this paper, the Operation Modal Analysis (OMA) has been used as an output-only technique for the calibration of the numerical model of the Collegiata.

3.1 Operational Modal Analysis

The OMA experimental campaign was carried out using four tri-axial Piezo-MEMS accelerometers connected to a SincHub for the synchronization. The sensors featured a sensitivity of 1V/g, a frequency range of 0.8-100 Hz and a dynamic range of 120 dB. Due to the limited length of the cables and the inaccessibility of the apse, OMA was restricted to the bell-tower only. To identify the most meaningful dynamic characteristics of this part, the four sensors were placed according to five different set-ups, maintaining the top two sensors as reference channels throughout the tests (Figure 4). Each measurement was recorded with a sampling frequency of 1024 Hz for a total duration of 45 minutes, resulting in 2.764.800 datapoints per channel.

Figure 4 Layout of the accelerometers in the tower

The acceleration time histories were then imported as output nodal processes in the ARTeMIS© software, after a pre-processing stage including filtering and decimation at 12.8Hz.

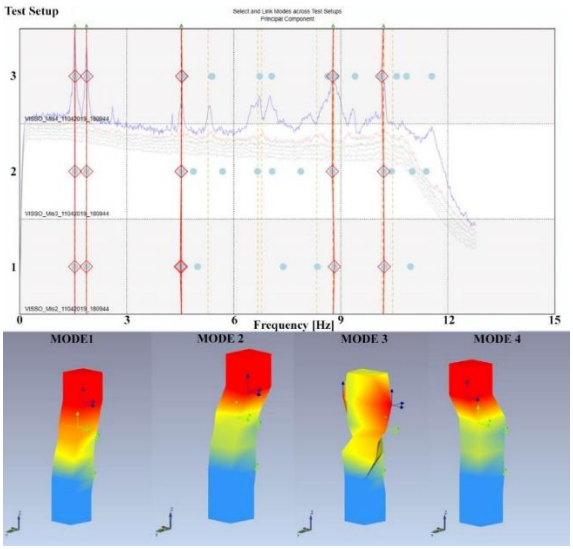

Figure 5 Stabilization diagram and experimental mode shapes of the tower identified with Cov-SSI method

The output-only modal parameter estimation was carried out according to the COVariance Stochastic Subspace Identification method (Cov-SSI) (Peeters & De Roeck, 1999) that works on output correlation for the estimation of the system's matrices and, therefore, of the eigen properties. This method operates directly in the time domain and is based on a state space formulation of the dynamic problem. The stabilization diagram obtained from the analysis of the collected data through Cov-SSI is reported in Figure 5 and allowed the determination of the *n* eigenvectors representative of the main structural modes (Table 1).

Table 1. Global modal properties of Collegiata di Visso's tower estimated via OMA.

Mode	f_{exp} (Hz)	ξ (%)	Complexity	Shape
1	1.55	0.75	0.23	TRAN-Y
2	1.87	1.07	0.28	TRAN-X
3	4.53	1.45	0.29	ROT-Z
4	8.79	1.84	0.78	FLEX-Y

3.2 Numerical modelling

With the aim of better understanding the structural response of the Collegiata of Visso, a Finite Element model was built in the MidasFea© software trying to reproduce as closely as possible the real geometry of the building. Afterward, the model was discretised with 4-node tetrahedral solid elements as shown in Figure 6, resulting into a model with 55107 elements, 16528 nodes and 47841 degrees of freedom.

Figure 6 Axonometric view of the Collegiata di Visso numerical model.

As a first attempt, the material parameters reported in Table 2 were assigned to different parts of the model by referring to the values provided in the Italian Building Code (Ministero delle infrastrutture e dei trasporti, 2019; Ministero delle Infrastrutture e dei Trasporti, 2018)

Table 2 Initial material parameters assigned to the FE model.

Material	E [MPa]	υ	w [kN/m^3]
Solid bricks and lime mortar	1500	0.49	18
Disordered rubble stone	870	0.49	19
Squared block stone	2800	0.49	22
Rough blocks within the inner core	1230	0.49	20
Ashlars masonry	1740	0.49	21

Then, a standard modal analysis was carried out to evaluate the dynamic properties of this first FE model (Model A) and compare them with the ones estimated experimentally. Considering that OMA was limited to the bell-tower, only the modal displacements of this part were considered for the tuning. The numerical frequencies and mode shapes corresponding to the first four measured vibration modes are shown in Table 3 and Figure 7, respectively. In Table 3, the MAC values between corresponding numerical and experimental modes are also reported.

Table 3 Eigenfrequencies and modal participation factors of the numerical vibration modes (Model A) corresponding to the first four experimental modes.

Mode	f_{num} (Hz)	Δf f_{exp}-f_{num} (%)	Mass X (%)	Mass Y (%)	Mass Z (%)	MAC (%)
1	1.64	6.00	0.97	20.64	0.00	96.97
2	2.01	7.00	14.10	1.17	0.00	95.97
4	5.14	13.00	11.48	0.44	0.00	64.92
11	9.03	3.00	0.10	0.03	17.19	2.15

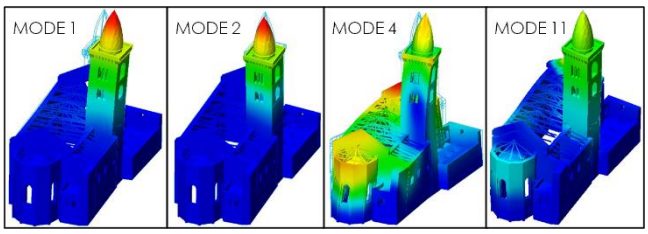

Figure 7 Numerical mode shapes (Model A).

As it can be seen, the numerical frequencies differ from the ones estimated experimentally, even if the first three modal shapes present similar configurations. To refine the calibration, changes were introduced in the model trying to better simulate the state of conservation of the different parts of the structure and paying attention to possible uncertainties (Model B). In particular, the mechanical parameters most influencing the dynamic response of the system were manually updated by successive steps. For the sake of brevity, only the fundamental steps that led to Model B, which appears to be the final calibrated model, will be listed hereafter. First of all, the presence of diffuse cracking along the tower – namely structural damage – was accounted for by reducing the Young's Modulus of the masonry in the affected part. This step permitted a tuning of the first two frequencies, but a big discrepancy still persisted for the higher modes. Thus, to enhance the tuning, it was necessary to simulate, adding rigid links, the effect of the interventions that took place following the Umbria-Marche earthquake of 1997 when, in addition to the new steel roof truss (already present in Model A given its good connection with the nave walls) r.c. slabs were added at the roof level of the sacristy and at the attics of the tower. The simulation of the diaphragm effect induced by the slabs, which soundly affects the overall behavior of the church, was fundamental for obtaining a good match between numerical and experimental higher frequencies. On the other side, the simulation of rigid floors led to a greater box-behavior, indeed in the last mode in addition to the bell-tower also the apse is involved. The presence of such floors allows more widespread damage to the part of the apse and, at the same time, permits to guarantee a higher MAC for the first three modes of the tower due to the reduction of the Young's Modulus on these elements. In Figure 8 the numerical mode shapes resulting from the last calibration step are reported, while the corresponding frequency values are summarized in Table 4 along with their experimental counterpart.

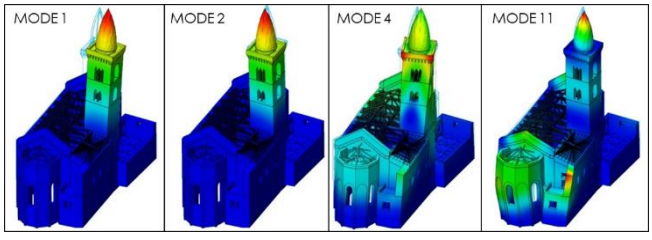

Figure 8 Numerical mode shapes (Model B).

Table 4 Experimental vs numerical frequencies after the calibration (Model B).

Mode	f_{exp} (Hz)	f_{num} (Hz)	Δf (%)	MAC (%)
1	1.55	1.55	0.06	96.36
2	1.87	1.82	2.83	95.52
4	4.53	4.75	4.97	79.02
11	8.80	8.99	2.16	35.89

4 OPTIMAL SENSOR PLACEMENT

With the aim of defining the optimal position and a minimum number of sensors necessary for the long-term structural health monitoring of the Collegiata, the mode shapes information obtained from the numerical model calibrated in Section 3 (Model B) were exploited to design the most appropriate sensor system network for the specific structure under analysis.

The sensor network design can be broken up into the definition of the following features: 1) quantities of interest, 2) observed quantities, 3) available instruments, 4) adopted optimization algorithm, 5) analyzed performance metrics. In the present study, quantities of interest are the modal properties of the system, aiming at tracking the dynamic behavior of the church over time and inferring damage-induced changes from their variations. Modal quantities can be estimated as from the nodal vibration responses measured through a set of uniaxial accelerometers, whose best placement definition is the main goal of this section.

The suitable algorithms for OSP can be classified as deterministic or stochastic, according to the way of addressing the system properties. Hereinafter, a deterministic approach is employed, namely the Effective Independence (EfI) method, which belongs to the so-called heuristic backward sequential sensor placement (BSSP) algorithms. BSSP are iterative approaches which carry out the optimization by rejecting at each step the sensor that contributes less to the maximization of a single specific performance metric. In this regard, the EfI developed by Kammer (Kammer, 1991) resorts to an index derived from the Fisher Information Matrix (FIM) as a performance metric to measure the mode identifiability. To support the modal identification, in fact, the measured mode shapes must be different enough otherwise their similarity can ill-condition the process of model updating. Aiming at the modal parameter correlation between experimental tests and FEM, Kammer (Kammer, 1991) was the first one to focus on this metric, being identifiability more restrictive than observability, which was addressed by the previous works in the field of control dynamics.

The FIM can be estimated according to the following formulation (Kammer, 1991):

$$FIM = E[(\boldsymbol{q} - \hat{\boldsymbol{q}})(\boldsymbol{q} - \hat{\boldsymbol{q}})^T]^{-1} = [\boldsymbol{\Phi_s}^T[\boldsymbol{\sigma}^2]^{-1}\boldsymbol{\Phi_s}] = P^{-1} \quad (1)$$

being:

$$\hat{\boldsymbol{q}}(t) = [\boldsymbol{\Phi_s}^{\mathrm{T}}\boldsymbol{\Phi_s}]^{-1}\boldsymbol{\Phi_s}^{\mathrm{T}}\boldsymbol{u_s}(t) \quad (2)$$

$$\boldsymbol{u_s} = \boldsymbol{\Phi_s}\boldsymbol{q} + \boldsymbol{N} \quad (3)$$

where E is the expected value, $\hat{\boldsymbol{q}}$ is the least squares estimate of the target modal coordinates $\boldsymbol{q}$ at the sensor locations, $\boldsymbol{\Phi_s}$ is the FE model mode shape matrix of the target modes, partitioned to the sensor locations, and $\boldsymbol{u_s}$ is the numerical simulated response measured by the sensors considering an error $\boldsymbol{N}$ in the output, assumed in the following as a random stationary Gaussian white noise with zero mean and $\boldsymbol{\sigma}^2$ variance, uncorrelated with identical statistical properties for each sensor. It results that the covariance matrix of the error P, namely the error between the state $\boldsymbol{q}$ and the estimate $\hat{\boldsymbol{q}}$, is the inverse of the FIM, thus maximizing the FIM leads to the best state estimate $\hat{\boldsymbol{q}}$. The EfI algorithm pursues this goal by calculating the effective independence distribution of the sensor set, $\boldsymbol{E_D}$:

$$\boldsymbol{E_D} = ([\boldsymbol{\Phi_s}\boldsymbol{\Psi}]\otimes[\boldsymbol{\Phi_s}\boldsymbol{\Psi}]\boldsymbol{\lambda}^{-1})\mathbf{1} \quad (4)$$

where $\boldsymbol{\Psi}$ and $\boldsymbol{\lambda}$ are the FIM eigenvectors and eigenvalues matrices, $\otimes$ is the term by term matrix multiplier and $\mathbf{1}$ is a column vector with all unitary elements. The ith term of the column vector $\boldsymbol{E_D}$ is assumed as the fractional contribution of the ith sensor to the linear independence of the modal partitions $\boldsymbol{\Phi_s}$. Considering that $0 \leq E_{Di} \leq 1$, the terms are sorted by magnitude and at any iteration the sensor with the lower value is rejected. After the rejection the effective independence value changes and the relevance of a sensor can change. Thus, the estimation must be repeated at any iteration.

The EfI method carries out the optimization focusing only on the FIM, but identifiability is fostered also by guaranteeing the orthogonality of the partitioned mode shape matrix. Therefore, in the present study, the performance metrics

reported in Table 5 are calculated and used to assess the sensor setup quality. In addition to the FIM, such metrics derive from the Singular Value Decomposition (SVD) of the power spectrum matrix (Penny, Friswell, & Garvey, 1994) and from the Modal Assurance Criterion matrix of the mode shape matrix (Penny et al., 1994) (Carne & Dohrmann, 1994):

$$MAC_{nm} = \frac{(\boldsymbol{\varphi}_n^{\mathrm{T}}\boldsymbol{\varphi}_m)^2}{(\boldsymbol{\varphi}_n^{\mathrm{T}}\boldsymbol{\varphi}_n)(\boldsymbol{\varphi}_m^{\mathrm{T}}\boldsymbol{\varphi}_m)} \quad (5)$$

where subscripts n, m refer to the columns of the FE model mode shape matrix of the target modes, partitioned to the sensor locations. Ideally the diagonal elements should be 1 and the off-diagonal should be 0.

Table 5: Sensor network performance metrics.

Performance metrics	Formulation
Trace of the FIM	$\mathrm{tr(FIM)} = \mathrm{tr}[\boldsymbol{\Phi}_s^{\mathrm{T}}\boldsymbol{R}^{-1}\boldsymbol{\Phi}_s]$
Determinant of the FIM	$\det(\mathrm{FIM}) = \det[\boldsymbol{\Phi}_s^{\mathrm{T}}\boldsymbol{R}^{-1}\boldsymbol{\Phi}_s]$
Max. off-diag. MAC	$\mathrm{MACmod} = \max_{n\neq m}\left(\frac{(\boldsymbol{\varphi}_n^{\mathrm{T}}\boldsymbol{\varphi}_m)^2}{(\boldsymbol{\varphi}_n^{\mathrm{T}}\boldsymbol{\varphi}_n)(\boldsymbol{\varphi}_m^{\mathrm{T}}\boldsymbol{\varphi}_m)}\right)$
SVD ratio	$\mathrm{SVDr} = \frac{\sigma_{max}}{\sigma_{min}}$

The OSP was carried out in MATLAB, resorting to a numerical tool firstly developed by C. Leyder (Leyder, Dertimanis, Frangi, Chatzi, & Lombaert, 2018), further enhanced and tested by the authors. As mentioned before, the last calibrated numerical model of the church (Model B) was employed for this purpose, defining a set of candidate locations easily accessible (Figure 9). Such locations correspond to the four corners of the tower at each floor level and to the window sills, plus 5 points belonging to the first floor of the sacristy. The first three numerical modes are targeted, presenting the lowest frequency percentage error and the highest MAC values in comparison with their experimental counterpart. For cost-efficient long-term monitoring, a minimum set of sensors able to maximize the information collected should be employed. Herein, the best deployments for a number of sensors variable between 3 and 6 are compared and the results are reported in Table 6.

As expected, the best candidate positions featured by the optimized sensor network correspond to the points located on the top floor of the tower. Indeed, looking at the performance metrics, it is possible to identify a significant deterioration of the performance when reducing the number of sensors from 4 to 3. The MACmod clearly shows it, providing a value close to 0.2 which, following (Carne & Dohrmann, 1994), is suggested to ensure that the vectors are distinguishable. In fact, even though theoretically any MAC value less than 1 identifies two vectors as distinct, comparing the same numerical and experimental vectors through a cross-MAC modelling error, measures error and uncertainties can turn the identification of the same modes extremely hard.

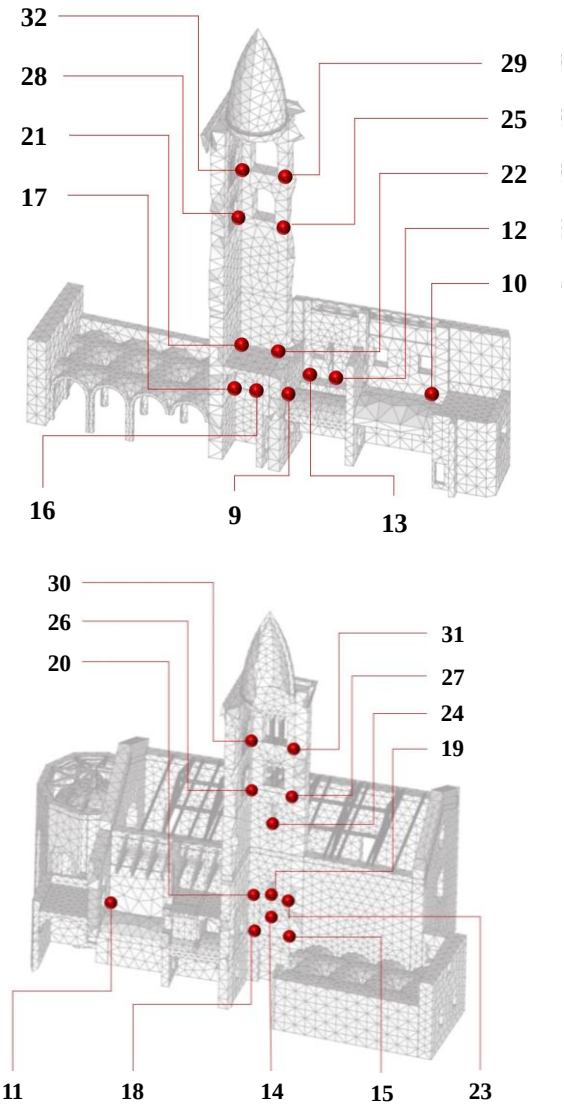

Figure 9 Candidate locations for OSP.

At the same time, the combination of MACmod and SVDr allows identifying deterioration of the algorithm performance even increasing sensors from 5 to 6, although a larger number of sensors provides more information as proved by the higher trace and determinant of the FIM. Altogether, the

SVDr metric allows to identify the best number of sensors as 4. The SVDr is the ratio of the largest to the smallest singular value of the mode shape matrix SVD. Since an orthogonal set of vectors leads to identical singular values, the closest the ratio to 1, the better the sensor placement. The highest performance of the network with 4 sensors can be also justified through the effective independence distribution of the different set-ups, reported in

Table 7. The values correspond to the fractional contribution of the *i* th sensor to the linear independence of the vectors in $\boldsymbol{\Phi_s}$. It is worth noting that the fractional contribution of all the nodes is above 0.5 when 4 sensors are deployed, but in case of 5 or more sensors, the contribution of some of them deteriorates, meaning that new added sensors are not relevant for the linear independence.

Table 6: OSP results.

N° sensors	Locations	Tr(FIM)	Det(FIM)	MACmod	SVDr
3	31x, 31y, 29y	4.67	2.47	0.16	1.94
4	32x, 31x, 31y, 29y	6.34	9.17	0.01	1.18
5	32x, 31x, 31y, 30y, 29y	7.65	15.63	0.01	1.28
6	32x, 31x, 31y, 30y, 29x, 29y	9.16	25.74	0.07	1.38

Table 7. Effective independence distribution of the sensor set.

N° node	6 sensors	5 sensors	4 sensors	3 sensors
32x	0.43	0.70	0.73	–
31x	0.64	0.70	0.73	1
31y	0.69	0.73	0.77	1
30y	0.41	0.41	–	–
29x	0.39	–	–	–
29y	0.44	0.45	0.77	1

5 CONCLUSIONS

The Collegiata of Santa Maria in Visso, the case of study of this paper, has been object of ambient vibration tests that allowed to identify the mode shapes and the principle frequencies characterizing the bell-tower. Using the results of the experimental campaign, a numerical model has been calibrated by updating specific mechanical parameters and paying attention to the actual state of conservation of the church to minimize the differences between measured and simulated responses. Indeed, it was necessary to reduce the elastic module in the masonry walls affected by serious cracks after the 2016-2017 earthquake, as the bell-tower and the apse, and add rigid links in the floors where the 2007 improvement interventions were carried out. After that, in view of a future long-term monitoring, an Optimal Sensors Placement algorithm was applied, using the first three vibration modes that presented the highest MAC value. At the start, several nodes located in accessible areas have been identified as possible candidate locations in the numerical model. The study has found that, out of all the accessible positions, only three corners on the tower's last floor are essential to obtain an adequate and reliable number of data for the long-time monitoring of the building, and that the necessary number of monoaxial accelerometers is four, two in node 32(x and y directions), one in node 31(x direction) and one in node 29 (y direction).

REFERENCES

Capellari, G., Chatzi, E., & Mariani, S. (2018). Structural Health Monitoring Sensor Network Optimization through Bayesian Experimental Design. *ASCE-ASME Journal of Risk and Uncertainty in Engineering Systems, Part A: Civil Engineering*, *4*(2), 04018016. https://doi.org/10.1061/AJRUA6.0000966

Carne, T. G., & Dohrmann, C. R. (1994). *A modal test design strategy for model correlation*. Sandia National Labs., Albuquerque, NM (United States).

Cavalagli, N., Comanducci, G., & Ubertini, F. (2018). Earthquake-Induced Damage Detection in a Monumental Masonry Bell-Tower Using Long-Term Dynamic Monitoring Data. *Journal of Earthquake Engineering*, *22*(sup1), 96–119. https://doi.org/10.1080/13632469.2017.1323048

Clementi, F., Pierdicca, A., Formisano, A., Catinari, F., & Lenci, S. (2017). Numerical model upgrading of a historical masonry building damaged during the 2016 Italian earthquakes: the case study of the Podestà palace in Montelupone (Italy). *Journal of Civil*

Structural Health Monitoring, *7*(5), 703–717. https://doi.org/10.1007/s13349-017-0253-4

Clementi, Francesco, Ferrante, A., Giordano, E., Dubois, F., & Lenci, S. (2019). Damage assessment of ancient masonry churches stroked by the Central Italy earthquakes of 2016 by the non-smooth contact dynamics method. *Bulletin of Earthquake Engineering*. https://doi.org/10.1007/s10518-019-00613-4

Ferraioli, M., Miccoli, L., & Abruzzese, D. (2018). Dynamic characterisation of a historic bell-tower using a sensitivity-based technique for model tuning. *Journal of Civil Structural Health Monitoring*, *8*(2), 253–269. https://doi.org/10.1007/s13349-018-0272-9

Giordano, E., Clementi, F., Nespeca, A., & Lenci, S. (2019). Damage Assessment by Numerical Modeling of Sant'Agostino's Sanctuary in Offida During the Central Italy 2016–2017 Seismic Sequence. *Frontiers in Built Environment*, *4*. https://doi.org/10.3389/fbuil.2018.00087

Guo, H. Y., Zhang, L., Zhang, L. L., & Zhou, J. X. (2004). Optimal placement of sensors for structural health monitoring using improved genetic algorithms. *Smart Materials and Structures*, *13*(3), 528–534. https://doi.org/10.1088/0964-1726/13/3/011

Kammer, D. C. (1991). Sensor placement for on-orbit modal identification and correlation of large space structures. *Journal of Guidance, Control, and Dynamics*, *14*(2), 251–259. https://doi.org/10.2514/3.20635

Leyder, C., Dertimanis, V., Frangi, A., Chatzi, E., & Lombaert, G. (2018). Optimal sensor placement methods and metrics – comparison and implementation on a timber frame structure. *Structure and Infrastructure Engineering*, *14*(7), 997–1010. https://doi.org/10.1080/15732479.2018.1438483

Li, B., Li, D., Zhao, X., & Ou, J. (2012). Optimal sensor placement in health monitoring of suspension bridge. *Science China Technological Sciences*, *55*(7), 2039–2047. https://doi.org/10.1007/s11431-012-4815-8

Masciotta, M. (2018). *OR CO*. 1–25. https://doi.org/10.1016/b978-0-08-102110-1.00008-x

Ministero delle infrastrutture e dei trasporti. (2019). Circolare 21 gennaio 2019 n. 7 C.S.LL.PP. Istruzioni per l'applicazione dell'aggiornamento delle "Norme Tecniche per le Costruzioni" di cui al D.M. 17/01/2018 (in Italian). *Suppl. Ord. Alla G.U. n. 35 Del 11/2/19*.

Ministero delle Infrastrutture e dei Trasporti. (2018). *DM 17/01/2018 - Aggiornamento delle "Norme Tecniche per le Costruzioni" (in italian)*. 1–198.

Monni, F., Clementi, F., Quagliarini, E., Giordano, E., & Lenci, S. (2017). Seismic Assessment of Cultural Heritage: Nonlinear 3d Analyses of "Santa Maria Della Carità" in Ascoli Piceno. *Proceedings of the 6th International Conference on Computational Methods in Structural Dynamics and Earthquake Engineering (COMPDYN 2015)*, 2533–2541. https://doi.org/10.7712/120117.5586.18082

Peeters, B., & De Roeck, G. (1999). Reference-Based Stochastic Subspace Identification for Output-Only Modal Analysis. *Mechanical Systems and Signal Processing*, *13*(6), 855–878. https://doi.org/10.1006/mssp.1999.1249

Penny, J. E. T., Friswell, M. I., & Garvey, S. D. (1994). Automatic choice of measurement locations for dynamic testing. *AIAA J.*, *32*, 407.

Pierdicca, A., Clementi, F., Isidori, D., Concettoni, E., Cristalli, C., & Lenci, S. (2016). Numerical model upgrading of a historical masonry palace monitored with a wireless sensor network. *International Journal of Masonry Research and Innovation*, *1*(1), 74. https://doi.org/10.1504/IJMRI.2016.074748

Quagliarini, E., Maracchini, G., & Clementi, F. (2017). Uses and limits of the Equivalent Frame Model on existing unreinforced masonry buildings for assessing their seismic risk: A review. *Journal of Building Engineering*, *10*, 166–182. https://doi.org/10.1016/j.jobe.2017.03.004

Worden, K., & Burrows, A. . (2001). Optimal sensor placement for fault detection. *Engineering Structures*, *23*(8), 885–901. https://doi.org/10.1016/S0141-0296(00)00118-8